$$t^L_{m'm} = (-)^L t^L_{m'-m}, \qquad m \text{ even} \tag{3.101}$$

3.3.4. The Texture-Free Mössbauer Spectrum of Thin Absorbers

The intensities of the spectra of thin absorbers are proportional to their thickness [equation (3.49)], so that the average of spectra measured at different γ-directions is equivalent to the average of the absorber matrices. This fact has been applied by Greneche and Varret[35] to obtain a random powder spectrum. They showed by doing an explicit calculation that the average of four spectra measured at appropriate directions of any absorber is identical with the spectrum of a random powder of the compound. The γ-directions are given by $\{\boldsymbol{\vartheta}_k;\ \vartheta = \arccos(1/\sqrt{3}),\ \varphi = k(\pi/2),\ k = 1,2,3,4\}$, where the arbitrary z axis may be chosen to be normal to the absorber plane.

This behavior is easily proved by group theoretical arguments within the framework of the theory presented. The different orientations of the absorber are described by the transformed texture components according to equation (3.90). This means that we arrive at an equation similar to equation (3.95) where the texture components of equivalent sites are calculated:

$$\tau^L_{m'm} = \sum_{k,n} D^L(\boldsymbol{\vartheta}_k)^+_{nm'} t^L_{nm} \tag{3.102}$$

Again we conclude that $\tau^L_{m'm}$ vanishes if the identity representation A_{1g} does not belong to the irreducible representation of the point group defined by the transformations $\{\boldsymbol{\vartheta}_k\}$. The four transformations given by Greneche and Varret can already be considered as the 24 transformations of the cubic group. The four γ-directions are parallel to the threefold rotation axes. For an unpolarized source the threefold rotation of the absorber gives the same spectra and therefore need not be carried out. The same argument holds for the inverted γ-direction by the twofold axes of the cubic group. Now we remember that for a dipole transition only texture components with $L = 2$ are measured, which have no A_{1g} representation in the cubic group. With these arguments we can propose a procedure with three measurements. We take the z axis, which may again be chosen normal to the absorber plane, as the threefold axis. Then the three angles are $\{\boldsymbol{\vartheta}_k;\ \vartheta = \arccos(1/\sqrt{3}),\ \varphi = 0, \pm 2\pi/3\}$ and the γ-direction is parallel to the fourfold axis of the cubic group.

The angle $\vartheta = \arccos(1/\sqrt{3}) = 54.7°$ is often called the magic angle[36]. If the texture has already an axial symmetry around the absorber axis then obviously only one measurement at this magic angle is necessary to obtain the powder intensities.

We may ask for the equivalent problem of an $E2$ transition where texture components up to $L = 4$ are involved. An inspection of the point groups shows that there is no invariant for $L \leq 6$ with respect to the transformations of the icosahedral group. Then the powder spectrum is obtained as the average of six measurements in the directions $\{\boldsymbol{\vartheta}_k;\ \vartheta = \arccos(1/\sqrt{5}),\ \varphi = (2\pi/5)k,\ k = 1,2,\ldots,5,\ \boldsymbol{\vartheta}_6 = 0\}$. The magic angle is $\vartheta = 63.4°$. For an axial texture two measurements have to be performed, one at $\vartheta = 0$ and one at the magic angle weighted by 1 and 5, respectively.

3.4. Goldanskii–Karyagin Effect

The anisotropic Debye–Waller factor f gives rise to anomalous intensities. In the case of a random powder absorber the anomaly was first observed by Goldanskii *et al.*[17] The equations for single crystals and textured powder absorbers will be evaluated in this section. The f factor implies some information which may also be of chemical interest.[36] This information is based on the fact that for molecular crystals the intramolecular vibrations are to a good approximation decoupled from the intermolecular vibrations, so that the f factor can be separated into two factors, the f factor of the crystal lattice f_C and of the molecule f_M giving $f = f_C \cdot f_M$. The mean square displacements $\langle r^2 \rangle$ of the intramolecular vibrations are responsible for f_M. They depend on the masses and the oscillator frequencies of the molecule and therefore are related to the bond strength.

The description of the combined effect of the texture and an anisotropic Debye–Waller factor on the intensities leads to a new type of the texture components which will be called super-texture components $\theta^L_{m'm}$. If the f factor is isotropic $f(\mathbf{k}) = \bar{f}(\mathbf{k})$ the super-texture components are the product of f and $t^L_{m'm}$: $\theta^L_{m'm} = t^L_{m'm} \cdot f$. The average of the absorber matrix will generally be obtained by replacing the $t^L_{m'm}$ by the quotient $\theta^L_{m'm}/\bar{f}(\mathbf{k})$.

3.4.1. The Super-Texture Components

If a single type of nucleus is considered the PAS of the EFG of which is oriented according to Figure 4a, the texture components with respect to S^γ are given by

$$t^L_{m'm}(\boldsymbol{\beta}) = (2L + 1)D^L(\boldsymbol{\beta})^+_{mm'} \tag{3.103}$$

The Euler angles $\boldsymbol{\beta}$ rotate S^γ to S^E as the angles $\boldsymbol{\theta}_k$ do in equation (3.94). The Debye–Waller factor f with respect to the system S^E has been defined in equation (3.2) by these angles $\boldsymbol{\beta}$

$$f(S^E,\boldsymbol{\beta}) = \sum_{Lm} f^L_m(S^E)D^L(0,\ \beta,\ \gamma)_{0m}$$

The super-texture components are defined by

$$\theta^L_{m'm}(\boldsymbol{\beta}) = t^L_{m'm}(\boldsymbol{\beta})f(S^E,\boldsymbol{\beta}) \tag{3.104}$$

For a textured powder sample or a single crystal with different equivalent sites $\theta^L_{m'm}$ has to be averaged by the corresponding texture function $T(\boldsymbol{\beta})$ which describes the texture of the absorber with respect to S^γ

$$\theta^L_{m'm} = \frac{1}{\Omega}\int \theta^L_{m'm}(\boldsymbol{\beta})T(\boldsymbol{\beta})\,d\boldsymbol{\beta} \tag{3.105}$$

By use of equation (3.72) $\theta^L_{m'm}$ gives

$$\begin{aligned}\theta^L_{m'm} = (2L+1) \sum_{L',L'',k} (-)^{m+m'} &\begin{pmatrix} L & L' & L'' \\ -m' & m' & 0 \end{pmatrix} \\ \times &\begin{pmatrix} L & L' & L'' \\ -m & k & m-k \end{pmatrix} t^{L'}_{m'k} f^{L''}_{m-k}(S^E)\end{aligned} \tag{3.106}$$

θ^0_{00} is the average of the f factor in accordance with the definition in equation (3.38b). The combined effect of texture and an anisotropic f factor leads to an infinite sum of products of both expansion coefficients. The simple transformation property of the texture components is not valid for the super-texture components. As a result the A_{Lm} values no longer transform as tensor components if the texture components $t^{L'}_{m'm}$ are replaced by the super-texture components divided by the average $\bar{f}$ of the f factor: $\theta^L_{m'm}/\bar{f}$. The rotated absorber can, however, again be treated as an absorber with the transformed texture components $t^{L'}_{k'k}(\boldsymbol{\vartheta}) = \Sigma_j t^{L'}_{jk} \mathrm{D}^{L'}(\boldsymbol{\vartheta})_{jk'}$ [equation (3.90)]. Inserting this transformation equation in equations (3.106) and (3.77) and rearranging the sums, the tensors $\tilde{A}_{L't}$, $\tilde{B}_{L't}$ can be constructed, the components of which determine the angular dependence of the absorber matrix in analogy to equation (3.80):

$$\bar{f}(\boldsymbol{\vartheta})\bar{r}_{pq}(\boldsymbol{\vartheta}) = \sum_{L't} \tilde{A}_{L't} D^{L'}(\boldsymbol{\vartheta})_{tq-p}, \qquad p-q = 0 \tag{3.107a}$$

In the equation for $p-q = \pm 2$ the tensor $\tilde{A}_{L't}$ is replaced by $\tilde{B}_{L't}$. The tensor $\tilde{A}_{L't}$ is given by

$$\tilde{A}_{L't} = \sum_{L,L'',m,k} a_m^L \begin{pmatrix} L & L' & L'' \\ -q+p & q-p & 0 \end{pmatrix}$$
$$\times \begin{pmatrix} L & L' & L'' \\ -m & k & m-k \end{pmatrix} t_{tk}^{L'} f_{m-k}^{L''}, \qquad p-q = 0 \quad (3.107\text{b})$$

The tensor $\tilde{B}_{L't}$, where $p-q = \pm 2$, is obtained by replacing a_m^L by b_m^L. We will not make use of these tensors but directly apply equation (3.106) for some special cases. There are no examples in the literature where a systematic evaluation of these tensor components could be performed.

The Goldanskii–Karyagin effect is obtained for a random powder $t_{m'm}^L = \delta_{0L}$:

$$\theta_{m'm}^L = f_m^L(S^E)\delta_{m'0} \qquad (3.108)$$

The intensity depends only on the A_L tensor component A_{L0}; the other components vanish, so that the r matrix is proportional to the unit matrix. It does not, of course, depend on the γ direction as a result of the random powder property of the absorber.

For the 1/2 → 3/2 transition the Goldanskii–Karyagin effect may be hidden if the tensor component A_{20} also vanishes. From equation (3.82) the condition $A_{20} = 0$ gives

$$\sqrt{6} f_0^2 + \eta(f_2^2 + f_{-2}^2) = 0 \qquad (3.109\text{a})$$

Expressed in Cartesian coordinates this condition is written as[15]

$$f_{zz} = \frac{1}{2}(f_{xx} + f_{yy}) - \frac{\eta}{2}(f_{xx} - f_{yy}) \qquad (3.109\text{b})$$

3.4.2. The Factorization of the Debye–Waller Factor

The expansion coefficients $f_m^L(S^E)$ of the Debye–Waller factor $f(S^E, \boldsymbol{\beta})$ of the Mössbauer nucleus shall be expressed by the coefficients $f_{C,m}^L(S^C)$ and $f_{M,m'}^{L'}(S^E)$ of the factors of the crystal lattice and the molecule, respectively. As a first step the expansion coefficients $f_{C,m}^L(S^C)$ referred to the crystal system S^C are given with respect to the system S^E. In a similar manner as in Section 3.3.2 it can be shown that

$$f_{C,m}^L(S^E) = \sum_n D^L(\boldsymbol{\theta})_{mn}^+ f_{C,n}^L(S^C) \qquad (3.110)$$

where $\boldsymbol{\theta}$ rotates S^C to S^E. The product

$$f_C(S^E,\boldsymbol{\beta})\cdot f_M(S^E,\boldsymbol{\beta}) = f(S^E,\boldsymbol{\beta}) \tag{3.111}$$

is explicitly written as

$$\sum_{L',m'} f^{L'}_{C,m'}(S^E)D^{L'}(\boldsymbol{\beta})_{0m'} \sum_{L'',m''} f^{L''}_{M,m''}D^{L''}(\boldsymbol{\beta})_{0m''} = \sum_{L,m} f^{L}_{m}(S^E)D^{L}(\boldsymbol{\beta})_{0m} \tag{3.112}$$

After replacing the product of the two rotation matrices by a series of rotation matrices[28] the comparison of the coefficients of $D^L_{0m}(\boldsymbol{\beta})$ on both sides gives

$$\begin{aligned} f^L_m(S^E) = (-)^m(2L+1) \sum_{L',L'',m',m''} &\begin{pmatrix} L & L' & L'' \\ 0 & 0 & 0 \end{pmatrix} \\ \times &\begin{pmatrix} L & L' & L'' \\ -m & m' & m'' \end{pmatrix} f^{L'}_{M,m'}(S^E) f^{L''}_{C,m''}(S^E) \end{aligned} \tag{3.113}$$

The Goldanskii–Karyagin effect of a random powder depends on the coefficients $f^L_m(S^E)$. In practice the infinite sum will be cut off at L' and L'' less than or equal to 4.

The average f factor of a random powder is f^0_0 [equation (3.108)]:

$$f^0_0(S^E) = \sum_{L',m'} (-)^{m'} f^{L'}_{M,m'}(S^E) f^{L'}_{C,-m'}(S^E)(2L'+1)^{-1} \tag{3.114}$$

It should be emphasized that this series is different from its first term $f^0_{M,0}\cdot f^0_{C,0}$, which is the product of the isotropic part of the f factors of the lattice and the molecule.

3.4.3. The Super-Texture Components of Single Crystals

Let the f factor be approximated by the product of the lattice part f_C and the molecule part f_M. The lattice part is the same for all Mössbauer nuclei in the lattice. For a single-crystal measurement f_C can be taken out of the sum of the general equation (3.107):

$$\begin{aligned} \theta^L_{m'm}(\boldsymbol{\vartheta}) &= f_C(-\boldsymbol{\vartheta})\cdot(2L+1)\cdot(-)^{m+m'} \\ &\times \sum_{L',L'',k',k,n} \begin{pmatrix} L & L' & L'' \\ -m & k' & 0 \end{pmatrix} \begin{pmatrix} L & L' & L'' \\ -m & k & n \end{pmatrix} t^{L'}_{k'k}(\boldsymbol{\vartheta}) \cdot f^{L''}_{M,n}(S^E) \end{aligned} \tag{3.115}$$

$\boldsymbol{\vartheta}$ rotates the crystal system S^C to the system S^γ. This is the opposite rotation as used for the angular dependence of the f factor in equation (3.2). Therefore, $\boldsymbol{\vartheta} = (\varphi, \vartheta, \psi)$ has to be replaced by $(-\psi, \vartheta, -\varphi) \equiv -\boldsymbol{\vartheta}$

in the f factor of the crystal: $f_C(-\vartheta)$. The average $\bar{f} = \theta^0_{00}$ of the f factor is still a complicated infinite sum:

$$\bar{f} = f_C(-\vartheta) \sum_{L',m} (-)^m \, t^{L'}_{0-m} f^{L'}_{M,m}(S^E) \frac{1}{2L' + 1} \tag{3.116}$$

An important case is the isotropic f factor of the molecule. The isotropy of f_M is a good approximation for low γ energies where f_M is in the vicinity of one.[38] Then $f_M \simeq f^0_{M,0}$ and equation (3.115) reduces to

$$\theta^L_{m'm} = f_C(-\vartheta) \cdot f^0_{M,0}(S^E) \cdot t^L_{m'm}(\vartheta) \tag{3.117}$$

so that $\theta^L_{m'm}/\bar{f} = t^L_{m'm}$. This situation has been referred to in Section 3.1.2 when discussing the applicability of the average of the intensity matrix.

Another case where only the texture components have to be applied is defined by a symmetry axis C_n which relates all n equivalent sites of the Mössbauer nuclei and leaves the arbitrary f factor at these sites invariant: $f_i(\mathbf{k}) = f_i(C_n\mathbf{k})$ at site i. This invariance holds for $\mathbf{k}$ parallel to the axis C_n or normal to a twofold axis C_2.

The infinite sum of equation (3.115) can, of course, always be avoided if instead of the integral in equation (3.105) with the texture function $T(\boldsymbol{\beta})$ the sum over the n equivalent sites is carried out explicitly:

$$\theta^L_{m'm} = \frac{1}{n} \sum_{i=1}^{n} t^L_{m'm}(\boldsymbol{\beta}_i) f(S^E, \boldsymbol{\beta}_i) \tag{3.118a}$$

The n values $f(S^E, \boldsymbol{\beta}_i)$ can all be identical or form groups of identical values as a result of the symmetry of the crystal. The former case has already been described above. Whether the exact equation (3.118a) or a limited series of equation (3.115) is preferred depends on the symmetry of the crystal, the number of equivalent sites, and the degree of anisotropy of the Debye–Waller factor f_M.

The $A_{Lm'}$ values are obtained by equation (3.77):

$$\bar{f} A_{Lm'} = \sum_m a^L_m \theta^L_{m'm} (2L + 1)^{-1}$$

If we define the $A_{Lm'}$ of a single site $A_{Lm'}(i) = \Sigma_m a^L_m t^L_{m'm}(\boldsymbol{\beta}_i)(2L + 1)^{-1}$ the components $A_{Lm'}$ are written as an average

$$\bar{f} A_{Lm'} = \frac{1}{n} \sum_{i=1}^{n} A_{Lm'}(i) f(S^E, \boldsymbol{\beta}_i) \tag{3.118b}$$

where $\bar{f} = (1/n)\,\Sigma^n f(S^E,\boldsymbol{\beta}_i)$. The $A_{Lm'}(i)$ transform as tensor components but the averages $A_{Lm'}$ do not. In most cases this formula [equation (3.118b)] will be applied (see Section 5.2.1c).

4. *Application of the Theory to Thin Absorbers*

This section deals with thin absorbers and unpolarized sources, the most common case of a Mössbauer experiment. Neither the convolution integral nor the density matrix formalism has to be applied evaluating the measured spectra. So we start with the formula of the area of an absorption line of the transition from the excited state $|I_e e_\beta\rangle$ to the ground state $|I_g g_\alpha\rangle$ [equation (3.49b)]:

$$A^{\alpha\beta} = f_s t\,\frac{\Gamma\pi}{2}\cdot\frac{1}{2}\,\mathrm{Tr}(\bar{r}^{\alpha\beta})$$

Since the diagonal elements $\bar{r}_{ii}^{\alpha\beta}$ ($i = \pm 1$) are the same for the pure quadrupole interaction under consideration, the area is determined by one absorber matrix element: $\bar{r}_{11}^{\alpha\beta}$. The basic idea outlined in Section 3.3 is the description of the angular dependence of the absorber matrix elements by the transformation properties of tensor components [equation (3.80)]:

$$\bar{r}_{11}^{\alpha\beta}(\vartheta) = \sum_{L,n} A_{Ln}^{\alpha\beta} D_{n0}^{L}(\vartheta) \tag{4.1a}$$

For pure quadrupole interactions L is even and runs from zero to $2\cdot L'$, L' being the multipolarity of the transition. The tensor component $A_{Ln}^{\alpha\beta}$ themselves are a sum of products of the components $(a_m^L)^{\alpha\beta}$ depending on the hyperfine interaction and the texture components $t_{m'm}^L$ characterizing the absorber [equation (3.77)]:

$$A_{Ln}^{\alpha\beta} = \sum_m (a_m^L)^{\alpha\beta} t_{nm}^L\cdot(2L + 1)^{-1}$$

The reader who reads this section in the beginning as recommended in the Introduction, first should make himself familiar with the meaning of the texture components (Sections 3.3.2 and 3.3.3). The components $(a_m^L)^{\alpha\beta}$ which are expressed by V_{zz} and η of the EFG tensor are explicitly given for the Mössbauer transition under consideration in Section 3.3.1. As an illustration the intensity formula for a single ^{57}Fe site as reported by P. Zory[21] is deduced. The explicit expressions for the $A_{Lm}^{\alpha\beta}$ components [equation (3.83)]

$$A_{00}^{\pi,\sigma} = \frac{1}{2}, \qquad A_{2m}^{\pi,\sigma} = \pm\frac{1}{20\sqrt{6}}\left[\frac{\sqrt{6}t_{m0}^2 + \eta(t_{m2}^2 + t_{m-2}^2)}{(1+\eta^2/3)^{1/2}}\right]$$

are inserted into equation (4.1a). π and σ stand for the two sets (α, β) of the four transitions from a degenerate excited state to a degenerate ground state. The texture component of a single lattice site with respect to the PAS of the EFG tensor [equation (3.93b)] simply is given by

$$t_{m'm}^L = (2L + 1)\delta_{mm'}$$

We can also begin with equation (4.1a) at $\vartheta = 0$

$$\bar{r}_{11}^{\alpha\beta} = A_{00}^{\alpha\beta} + A_{20}^{\alpha\beta} + \cdots \tag{4.1b}$$

and use the transformation properties of the texture component. The texture components are transformed to the system S^γ (ϑ) of the direction of observation [equation (3.90b)] by

$$t_{m'm}^L(\vartheta) = \sum_n D^L(\vartheta)_{nm'} t_{nm}^L$$

With respect to PAS of the EFG tensor the equation reduces to

$$t_{m'm}^L(\vartheta) = (2L + 1)D^L(\vartheta)_{mm'}$$

Starting with equation (4.1a) as well as (4.1b) we obtain with the known rotation matrix elements the formula of Zory[21] for a single lattice site

$$R = \frac{4(1+\eta^2/3)^{1/2} + (3\cos^2\vartheta - 1) + \eta\sin^2\vartheta\cos2\varphi}{4(1+\eta^2/3)^{1/2} - (3\cos^2\vartheta - 1) - \eta\sin^2\vartheta\cos2\varphi} \tag{4.2}$$

where $R = \bar{r}_{11}^{\pi}/\bar{r}_{11}^{\sigma}$ is the intensity ratio of the π and σ transition.

The more complicated case of an anisotropic Debye–Waller factor leads to the definition of the super-texture components $\theta_{m'm}^L$ introduced in Section 3.4. They depend on the texture components and the coefficients f_m^L of the expansion series of the f factor [equation (3.2)]. The texture components $t_{m'm}^L$ in the equation above then have to be replaced by the quotient $\theta_{m'm}^L/\theta_{00}^0$. With the super-texture components of a random powder $\theta_{0m}^L = f_m^L$ [equation (3.108)] the Goldanskii–Karyagin effect[17,18] is immediately derived. Inserting f_m^2/f_0^0 instead of t_{0m}^2 in equation (4.1.b) the intensity ratio is given by

$$R = \frac{\frac{1}{2}f_0^0(1 + \eta^2/3)^{1/2} + [\sqrt{6}\, f_0^2 + \eta(f_2^2 + f_{-2}^2)]/20\sqrt{6}}{\frac{1}{2}f_0^0(1 + \eta^2/3)^{1/2} - [\sqrt{6}\, f_0^2 + \eta(f_2^2 + f_{-2}^2)]/20\sqrt{6}} \tag{4.3}$$

The first part of this section deals with powder absorbers and the second one with single crystals. It may be instructive first to read the application of this formalism on Zory's measurements of $FeCl_2 \cdot 4H_2O$ and its connection to the Cartesian intensity tensor of Zimmermann (Section 4.2.1). The evaluation of the measurements of single crystals of $KAu(CN)_2$ in Section 4.2.2 is more difficult as a result of the factorization of the f factor into an anisotropic lattice part and a local molecular part.

4.1. Powder Spectra

From the Mössbauer spectrum of a random powder only the invariants of the EFG tensor can be obtained. These are the quadrupole splitting $\Delta E_Q = |eQ|\sqrt{\phi_{II}}$ and ϕ_{III} or equivalently V_{zz} and η [see equations (1.17) and (1.19)]. The orientation of the EFG tensor remains unknown. But the relative orientation of the EFG tensor with respect to an anisotropic mean square displacement tensor (MSD tensor) enters in the equations of the intensities. This information is accessible if the Goldanskii–Karyagin effect is observed. The main part of this section deals with this effect. The consequences of a textured powder combined with the Goldanskii–Karyagin effect are also discussed.

4.1.1. The Random Powder and Isotropic Debye–Waller Factor

Let us first very briefly consider the spectra with an isotropic f factor. The $3/2 \rightarrow 1/2$ transitions show the two absorption lines of equal intensities with the separation ΔE_Q which defines the quadrupole splitting. η and the sign of V_{zz} are hidden parameters. Transitions involving higher nuclear spin states reveal the two invariants even if the spectra are poorly resolved. In Figure 5 the Mössbauer spectra at different temperatures of the $5/2^+ \rightarrow 7/2^+$ transition of ^{151}Eu are shown.[39] By comparison with the stick diagram of Figure 2 the asymmetry of the shape of the spectra immediately tells us that the scaling factor $\mu_{I_g} = eQ_gV_{zz}/[4I_g(2I_g - 1)]$ (see Section 2.2) is negative. The intensities of the pure dipole transitions in Figure 2 are proportional to the trace of the intensity matrices [see equation (3.66)] according to equation (3.74). The fits are obtained with $\eta = 0$ in agreement with the crystal structure of $Eu_2Ti_2O_7$, where the Eu sites lie on a threefold rotation axis. The accuracy of the quadrupole splitting is about 1% in spite of the poor resolution.

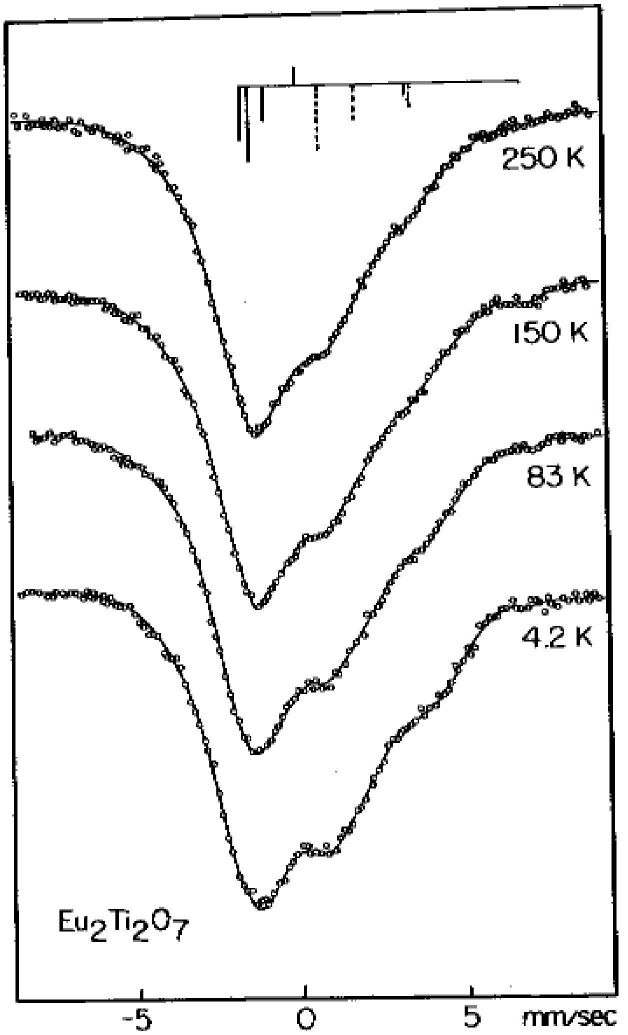

FIGURE 5. Mössbauer spectra of $Eu_2Ti_2O_7$. Positions of the eight transitions are shown at the top. The $\Delta m = 0$ transitions are indicated by the dashed lines (from Reference 39).

4.1.2. The Goldanskii–Karyagin Effect

Before the effect of an anisotropic f factor on the intensities is considered the expansion coefficients f^L_m are calculated for some special but frequently used cases. In the harmonic approximation a MSD tensor can be used. In the PAS of the second-rank tensor denoted by S^M we have

$$M = \begin{pmatrix} \langle x^2\rangle & & \\ & \langle y^2\rangle & \\ & & \langle z^2\rangle \end{pmatrix} \tag{4.4}$$

x,y,z are the amplitudes of the nuclear vibrations in the direction of coordinate axes of S^M. If $\mathbf{k} = k(\sin\vartheta\cos\varphi, \sin\vartheta\sin\varphi, \cos\vartheta)$ is the wave vector of the γ quanta with respect to S^M, the f factor for a harmonic lattice is given by

$$\begin{aligned} f &= \exp(-\mathbf{k}M\mathbf{k}) \\ &= \exp[-k^2(\cos^2\varphi\langle x^2\rangle + \sin^2\varphi\langle y^2\rangle)\sin^2\vartheta \\ &\quad - k^2\langle z^2\rangle\cos^2\vartheta] \end{aligned} \tag{4.5}$$

The expansion series of equation (3.2) uses the Euler angles $\gamma = \pi - \varphi$, $\beta = \vartheta$, so that $\mathbf{k} = k(-\sin\beta\cos\gamma, \sin\beta\sin\gamma, \cos\beta)$. The expansion coefficients of $f(\beta,\gamma) = \Sigma_{L,m} f^L_m D^L_{0m}(\beta,\gamma)$ are obtained by the integral

$$f^L_m = (2L+1)\frac{1}{\Omega}\int f(\beta,\gamma)D^L(\beta,\gamma)^+_{m0}\,d\Omega \tag{4.6}$$

It is easily shown by the symmetry of the MSD tensor, that L are even integers and $f^L_m = f^L_{-m}$. The special case of a MSD tensor of axial symmetry: $\langle x^2\rangle = \langle y^2\rangle \neq \langle z^2\rangle$ is realized in many crystals. With the anisotropy parameter

$$N = k^2(\langle z^2\rangle - \langle x^2\rangle) \tag{4.7}$$

the nonzero expansion coefficients are

$$f^L_0 = (2L+1)\exp(-k^2\langle x^2\rangle)\cdot\frac{1}{2}\int_0^\pi \exp(-N\cos^2\beta)P_L(\cos\beta)\sin\beta\,d\beta \tag{4.8}$$

In Figure 6 the ratios

$$\zeta^L_0 = f^L_0/f^0_0 \tag{4.9a}$$

and

$$\zeta = f^0_0/\exp[-\tfrac{1}{3}k^2(2\langle x^2\rangle + \langle z^2\rangle)] \tag{4.9b}$$

are plotted versus the anisotropy parameter N. For small N the exponential function may be expanded in a series and integrated:

$$f^0_0 = \exp(-k^2\langle x^2\rangle)\left(1 - \frac{1}{3}N + \frac{1}{10}N^2 - \cdots\right) \tag{4.10}$$

$$\left.\begin{aligned} f^2_0 &= \exp(-k^2\langle x^2\rangle)N\left(-\frac{2}{3} + \frac{2}{7}N - \cdots\right)\\ f^4_0 &= \exp(-k^2\langle x^2\rangle)N^2\left(\frac{4}{35} - \frac{4}{77}N + \cdots\right)\\ f^6_0 &= \exp(-k^2\langle x^2\rangle)N^3\frac{8}{99}\left(-\frac{1}{7} + \frac{1}{15}N - \cdots\right)\end{aligned}\right\} \tag{4.11}$$

Up to $N = 1$ these expressions are correct within 3%. The ratios ζ^L_0 are then calculated to be

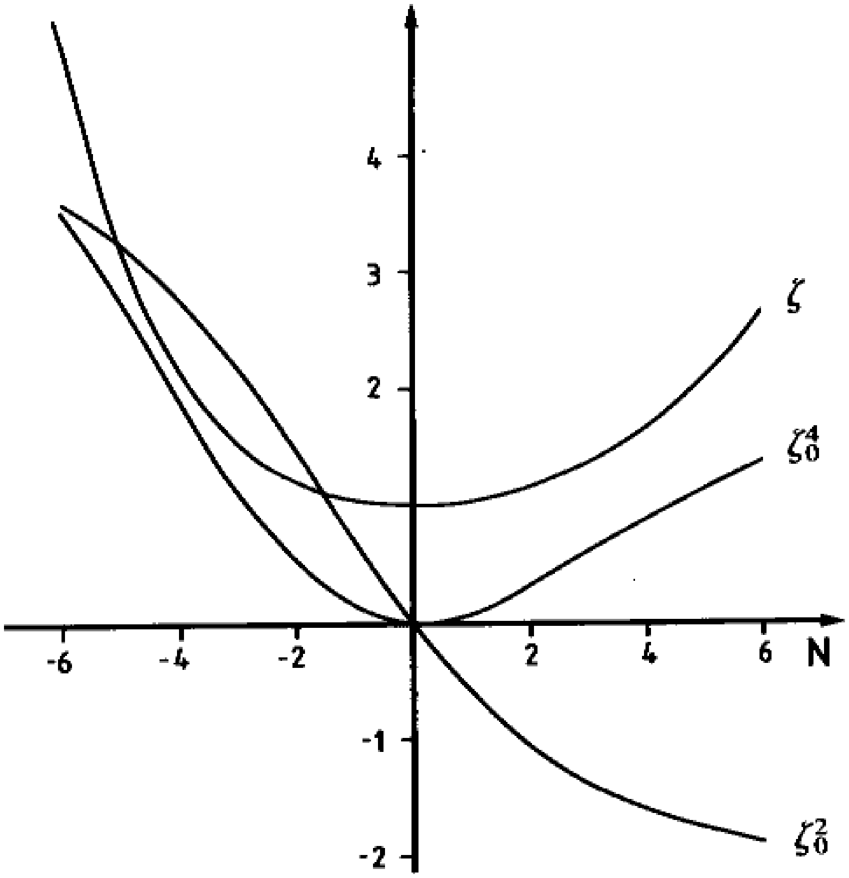

FIGURE 6. The ratio $f_0^L/f_0^0 = \zeta_0^L$ of the expansion coefficients $f_0^L(L = 2,4)$ of the Debye–Waller factor $f(\vartheta)$ are plotted versus the asymmetry parameter $N = k^2(\langle z^2\rangle - \langle x^2\rangle)$ of an axial MSD tensor. $\zeta(N)$ is defined by $\zeta(N) = f_0^0(N)/\exp[-\frac{1}{3}k^2(\langle x^2\rangle + \langle y^2\rangle + \langle z^2\rangle)]$.

$$\begin{aligned} \zeta_0^2 &= -\frac{2}{3}N\left(1 - \frac{2}{21}N + \cdots\right) \\ \zeta_0^4 &= \frac{4}{35}N^2\left(1 - \frac{4}{77}N + \cdots\right) \\ \zeta_0^6 &= -\frac{8}{693}N^3\left(1 - \frac{2}{35}N + \cdots\right) \end{aligned} \tag{4.12}$$

The f_0^0 component is the average value $\bar{f}$ of $f(\beta, \gamma)$. For small N the sum in equation (4.10) is approximately the same as $\exp(-N/3)$, so that with the definition of N the average f_0^0 is written as[40]

$$f_0^0 = \exp[-\tfrac{1}{3}k^2(2\langle x^2\rangle + \langle z^2\rangle)] \tag{4.13a}$$

or equivalently

$$-\ln f_0^0 = \tfrac{1}{3}(-\ln f_z - 2\ln f_x) \tag{4.13b}$$

where f_x and f_z are the f factors in the x and z directions, respectively. The first correction to the linear approximation of equation (4.13a) is given by the factor $[1 + (2/45)N^2]$, so that instead of equation (4.10) we can use

$$f_0^0 = \exp[-\tfrac{1}{3}k^2(2\langle x^2\rangle + \langle z^2\rangle)]\left(1 + \frac{2}{45}N^2 + \cdots\right) \tag{4.14}$$

To describe the nonaxial f factor we define a further anisotropy parameter

$$n = k^2(\langle y^2\rangle - \langle x^2\rangle) \tag{4.15}$$

Up to $L = 2$ the following expressions are evaluated to second order in N and n:

$$\begin{aligned} f_0^0 = \exp(-k^2\langle x^2\rangle)\bigg[& 1 - \frac{1}{3}(N + n) \\ & + \frac{1}{10}(N + n)^2 + \frac{1}{15}Nn + \cdots\bigg] \end{aligned} \tag{4.16a}$$

or

$$\begin{aligned} f_0^0 = \exp[-k^2(\langle x^2\rangle + \langle y^2\rangle + \langle z^2\rangle)]\bigg[& 1 + \frac{2}{45}(N + n)^2 \\ & + \frac{1}{15}Nn + \cdots\bigg] \end{aligned} \tag{4.16b}$$

$$\begin{aligned} f_0^2 &= \exp(-k^2\langle x^2\rangle)\,\frac{1}{21}[-7(2N - n) \\ &\qquad + 3(2N^2 - n^2) + nN + \cdots] \\ f_{\pm2}^2 &= \exp(-k^2\langle x^2\rangle)\,\frac{\sqrt{6}}{2}n(7 - N - 3n + \cdots) \end{aligned} \tag{4.17}$$

The ratios $f_m^L/f_0^0 = \zeta_m^L$ are given by

$$\begin{aligned} \zeta_0^2 &= -\frac{2}{3}N\left(1 - \frac{2}{21}N\right) + \frac{1}{3}n\left[1 - \frac{2}{21}(2N + n)\right] + \cdots \\ \zeta_{\pm2}^2 &= \frac{\sqrt{6}}{126}n\,(21 + 4N - 2n) + \cdots \end{aligned} \tag{4.18}$$

4.1.2a. The 3/2⁻ → 1/2⁻ Transition (M1) of ^{57}*Fe.* As a first example the Goldanskii–Karyagin effect in $FePS_3$ reported by R. Chandra and T. Ericsson[38] will be discussed. Figure 7 shows the powder Mössbauer spectra at three temperatures. The asymmetry of the ^{57}Fe quadrupole doublet increases with increasing temperature. This dependence clearly proves the presence of the Goldanskii–Karyagin effect. The evaluation of the information obtained from the asymmetry of the doublet will be repeated

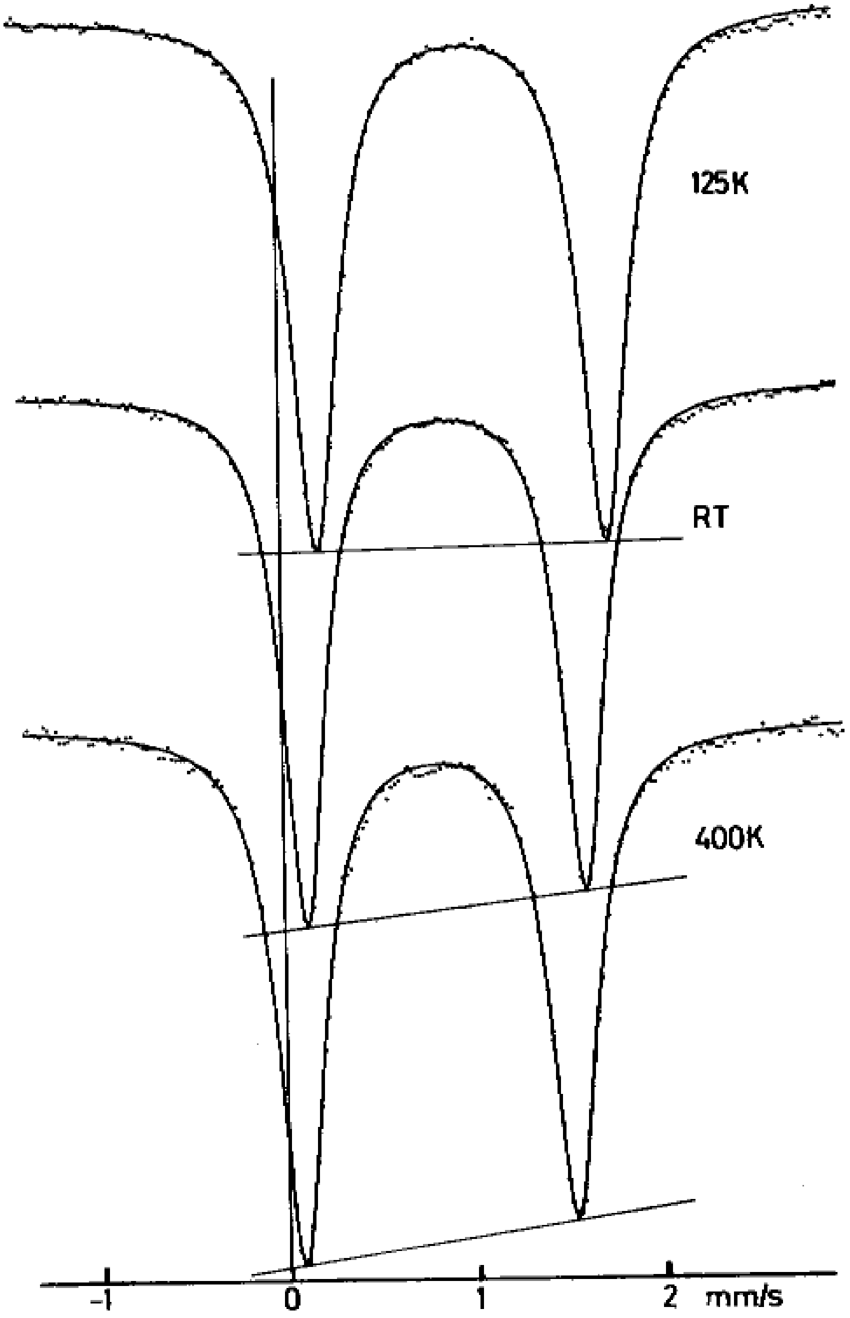

FIGURE 7. Mössbauer spectra of $FePS_3$ recorded at 125 K, room temperature, and 400 K. The asymmetry is visualized by straight lines through the peak positions (from Reference 38).

for one temperature ($T = RT$) in two different ways. In the beginning all assumptions of Chandra and Ericsson are used and afterwards a more general evaluation will be performed which takes into account only the crystal structure of the compound.

$FePS_2$ has a monoclinic structure, space group $C2/m$. There are four formula units in the unit cell. The iron atoms occupy only one site which lies on the twofold rotation axis b. The structure is repeated normal to the a,b plane after three monoclinic layers. From a point charge calculation the authors conclude that $V_{zz} > 0$, the z axis is almost normal to the a,b plane, and the asymmetry parameter η is close to zero. The MSD tensor has also been assumed to be axial, the symmetry axis being parallel to the z axis of the EFG tensor.

The intensity ratio $R = \bar{r}^{\pi}_{11}/\bar{r}^{\sigma}_{11}$ is written by use of equation (3.76) ($\bar{r}^{\pi}_{11} = 1 - \bar{r}^{\sigma}_{11}$) as

$$R = (\tfrac{1}{2} + A^{\pi}_{20})/(\tfrac{1}{2} - A^{\pi}_{20}) \tag{4.19}$$

so that $A^{\pi}_{20} = \frac{1}{2}(R-1)/(R+1)$. For the interpretation of the measurement the equation of A_{20} [equation (3.83)] has to be discussed. Inserting the super-texture components of a random powder [equation (3.108)] divided by $\bar{f}(=f^0_0)$ gives

$$A^{\pi}_{20} = \frac{1}{20\sqrt{6}}[\sqrt{6}\,\zeta^2_0 + \eta(\zeta^2_2 + \zeta^2_{-2})]/(1 + \eta^2/3)^{1/2} \tag{4.20}$$

The average f factor follows a Debye model[38] with $\theta \simeq 200$ K, so that $f^0_0(RT) = 0.35$. Assuming $\eta = 0$ the value of $R(RT) = 0.93$ leads to $\zeta^2_0 = -0.36$. From Figure 6 we obtain $N = 0.60$ and $\zeta \simeq 1.0$ so that $k^2(2\langle x^2\rangle + \langle z^2\rangle) = -3 \ln f^0_0 = 3.15$. The ratio of the mean square displacements of vibrations perpendicular and parallel to the a,b plane is then [equation (4.7)] given by $\langle z^2\rangle/\langle x^2\rangle = 1.70$. If we take the linear approximation of equation (4.12) and equation (4.14) the values $k^2\langle x^2\rangle = 0.87$ and $\langle z^2\rangle/\langle x^2\rangle = 1.62$ differ by only a few percent.

A more general evaluation of the data will take into account an arbitrary MSD tensor. The twofold symmetry axis of the crystal passes through the iron atoms. The EFG tensor and the MSD tensor therefore have one principal axis in common. This axis is chosen as the y axis for both tensors. The z axes of the two PAS systems S^E and S^M may include an angle θ. The expansion coefficients f^L_m are transformed to the PAS of the EFG by equation (3.110):

$$f^L_m(S^E) = \sum_n D^L(\theta)^+_{mn} f^L_n(S^M)$$

where $\boldsymbol{\theta} = (0, \theta, 0)$ rotates S^M to S^E. $f_0^0(S^E) = f_0^0(S^M) = f_0^0$ is invariant. For the coefficients $f_m^2(S^E)$ one obtains $[f_2^2(S^M) = f_2^2(S^M)]$

$$
\begin{aligned}
f_0^2(S^E) &= f_0^2(S^M) - \frac{\sqrt{6}}{4}\sin^2\theta[\sqrt{6}f_0^2(S^M) - 2f_2^2(S^M)] \\
f_{\pm 1}^2(S^E) &= \pm\sin\theta\cos\theta[-\tfrac{1}{2}\sqrt{6}f_0^2(S^M) + f_2^2(S^M)] \qquad (4.21) \\
f_{\pm 2}^2(S^E) &= f_2^2(S^M) + \tfrac{1}{4}\sin^2\theta[\sqrt{6}f_0^2(S^M) - 2f_2^2(S^M)]
\end{aligned}
$$

Therefore, the measured value A_{20}^{π} of equation (4.20) defines interrelations between the four parameters η, θ, $\zeta_0^2(S^M)$, $\zeta_2^2(S^M)$:

$$
\begin{aligned}
A_{20}^{\pi} = \frac{1}{20(1 + \eta^2/3)^{1/2}} \{&\zeta_0^2(S^M)[1 - \tfrac{1}{2}(3 - \eta)\sin^2\theta] \\
&+ \sqrt{\tfrac{2}{3}}\zeta_2^2(S^M)[\eta + \tfrac{1}{2}(3 - \eta)\sin^2\theta]\} \qquad (4.22)
\end{aligned}
$$

The values ζ_0^2 and ζ_2^2 are expressed by the anisotropy parameters N and n according to equation (4.18). We will consider the case of vanishing η and θ, which is suggested by the point charge calculation and the layer structure of the compound. In the linear approximation of equation (4.18) we obtain

$$
A_{20}^{\pi} = \frac{1}{20}\left[-\frac{1}{3}(2N - n)\right] \qquad (4.23)
$$

The factor $2N - n = k^2[2\langle z^2\rangle - (\langle x^2\rangle + \langle y^2\rangle)]$ shows that only the average of the components of the MSD tensor in the a,b plane can be measured in accordance with the tensor property of f itself in the linear approximation. The expansion to second order in n and N reveals a dependence on $\langle x^2\rangle$ and $\langle y^2\rangle$ separately. To give one example we take $n = N/2$ and obtain $k^2\langle x^2\rangle = 0.73$, $k^2\langle y^2\rangle = 1.09$, $k^2\langle z^2\rangle = 1.50$. The mean square displacements in the a,b plane then differ by a factor of 1.5. The ratio $\langle z^2\rangle$ divided by the average $\frac{1}{2}(\langle x^2\rangle + \langle y^2\rangle)$ gives 1.65, which is almost the same value as for an axial MSD tensor (1.70) where $n = 0$. However, at higher energies of the γ rays (other Mössbauer isotopes) the N,n values increase beyond the range where the linear approximation is sufficient.

4.1.2b. The $5/2^+ \rightarrow 7/2^+$ Transition of ^{151}Eu in $Eu_2Ti_2O_7$. The Mössbauer spectra at lower temperatures of the $5/2^+ \rightarrow 7/2^+$ magnetic dipole transition of ^{151}Eu in the compound $Eu_2Ti_2O_7$ have already been shown in Figure 5. At higher temperatures a pronounced Goldanskii–Karyagin effect is observed.[41] In Figure 8 the dashed lines are theoretical spectra

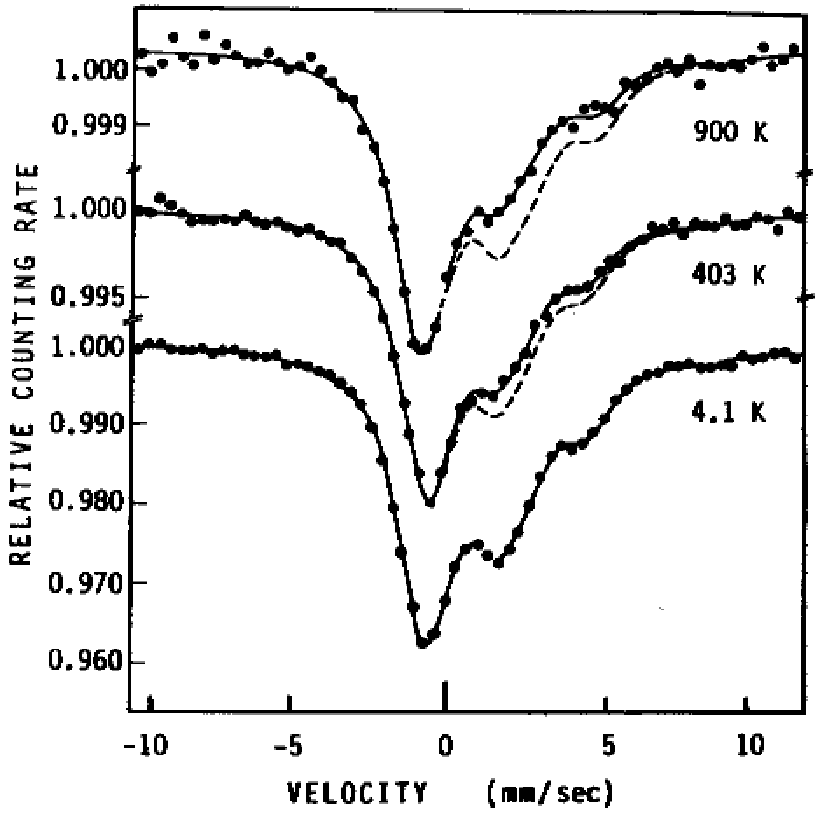

FIGURE 8. Recoilless absorption spectra of the 21.6-keV gamma rays of ^{151}Eu in $Eu_2Ti_2O_7$. The solid lines are the theoretical spectra obtained from least-squares computer fits to the experimental spectra, taking into account an anisotropic absorption fraction. The dashed lines are theoretical spectra obtained with isotropic absorption fraction (from Reference 41).

obtained with an isotropic absorption fraction. The solid lines are least-squares computer fits to the experimental spectra. The fits were obtained by multiplying the relative intensities of all $\Delta m = 0$ transitions (given by the appropriate powder intensities) by a reduction factor B: $B(400\ K) = 0.73$ and $B(900\ K) = 0.56$. The connection of this factor B to the components of the MSD tensor is unique in this case as a result of the symmetry of the lattice. The pyrochlore compounds $Eu_2Ti_2O_7$ have the space group $Fd\bar{3}m$ and the Eu^{3+} occupy a threefold symmetry site ($\bar{3}m$ symmetry). Therefore, the MSD tensor of the Eu ion has axial symmetry and the PASs of the EFG tensor and the MSD tensor coincide. In the approximation where the f factor can be written as the product $f_C \cdot f_M$ the f factor of the cubic crystal is isotropic and the local f factor of the molecule anisotropic. This factorization is, however, fictitious since there is principally no way to determine the factors separately. The relation between the factor B and the expansion coefficient f_m^L of the Debye–Waller factor is deduced in the following.

Inserting the super-texture components of a random powder [equation

(3.106)] in equation (3.77a) of the A_{Lm}, the absorber matrix component $\bar{r}_{11} = A_{00} + A_{20}$ is written as

$$\bar{r}_{11} = a_{00} + \sum_m a^2_m \zeta^2_m/5 \tag{4.24}$$

The a^2_m are expressed by the components of intensity matrices [equation (3.78)]:

$$\bar{r}_{11} = \tfrac{1}{3}\mathrm{Tr}(I^1) + \frac{1}{15}(I^1_{11} - I^1_{00})\zeta^2_0 + \frac{2}{5\sqrt{6}} I^1_{1-1}\zeta^2_2 \tag{4.25}$$

For an axially symmetric EFG tensor the diagonal I matrices are given in equation (3.66). With the identity $I^1_{11} - I^1_{00} = \tfrac{1}{2}\mathrm{Tr}(I^1) - \tfrac{3}{2}I^1_{00}$ equation (4.25) becomes

$$\bar{r}_{11} = \tfrac{1}{3}\mathrm{Tr}(I^1)(1 + \tfrac{1}{10}\zeta^2_0) - \tfrac{1}{10}I_{00}\zeta^2_0 \tag{4.26}$$

Of the eight matrices of equation (3.66) five belong to a pure $\Delta m = \pm 1$ transition ($I^1_{00} = 0$) and two belong to a $\Delta m = 0$ transition [$\mathrm{Tr}(I) = I_{00}$]. The matrix $I^1(1,1) = (3/28, 3/4, 3/28)$ contains both transitions. It shall be considered as a sum of two matrices: $I^\pi(1,1) = (3/28, 0, 3/28)$ and $I^\sigma(1,1) = (0, 3/7, 0)$. Then equation (4.26) can be simplified to two types of equations:

$$\bar{r}_{11}(\pi) = \tfrac{1}{3}\mathrm{Tr}(I^1)(1 + \tfrac{1}{10}\zeta^2_0) \tag{4.27a}$$

$$\bar{r}_{11}(\sigma) = \tfrac{1}{3}\mathrm{Tr}(I^1)(1 - \tfrac{1}{5}\zeta^2_0) \tag{4.27b}$$

There are now six π transitions ($\Delta m = \pm 1$) and three σ transitions ($\Delta m = 0$) where two of them have the same transition energy. $\tfrac{1}{3}\mathrm{Tr}(I)$ is the intensity of the random powder [equation (3.74)]. The factors $1 + \zeta^2_0/10$ and $1 - \zeta^2_0/5$ give rise to the Goldanskii–Karyagin effect. In the thin absorber approximation a common factor multiplied to all intensities does not change the relative intensities. If $1/(1 + \zeta^2_0/10)$ is taken as such a factor the σ transitions appear to be changed by the factor

$$B = \frac{1 - \zeta^2_0/5}{1 + \zeta^2_0/10} \tag{4.28a}$$

$$\zeta^2_0 = 10(1 - B)/(2 - B) \tag{4.28b}$$

This factor B is usually determined experimentally. For our example B(400 K) = 0.73 gives $\zeta^2_0 = 2.13$ so that $N = -2.86$ is derived from Figure 6.

4.1.2c. The $2^+ \rightarrow 0^+$ Transition of ^{156}Gd in $Gd_2Ti_2O_7$. As a result of the approximately four times larger transition energy of the 89-keV Mössbauer transition of ^{156}Gd as compared with the 21.6-keV transition of ^{151}Eu the anisotropy factor $N = k^2(\langle z^2\rangle - \langle x^2\rangle)$ will be enlarged considerably. Neglecting the small mass difference between the two Mössbauer atoms which slightly influence the MSD amplitudes of the same crystal structures N will be enlarged by a factor of $\simeq 16$, so that a pronounced Goldanskii–Karyagin effect is expected. Figure 9 shows the Mössbauer spectra of $Gd_2Ti_2O_7$ at $T = 4.2$ K and $T = 70$ K.[42] The dashed curves calculated with an isotropic f factor are very different from the measured spectra even at 4.2 K.

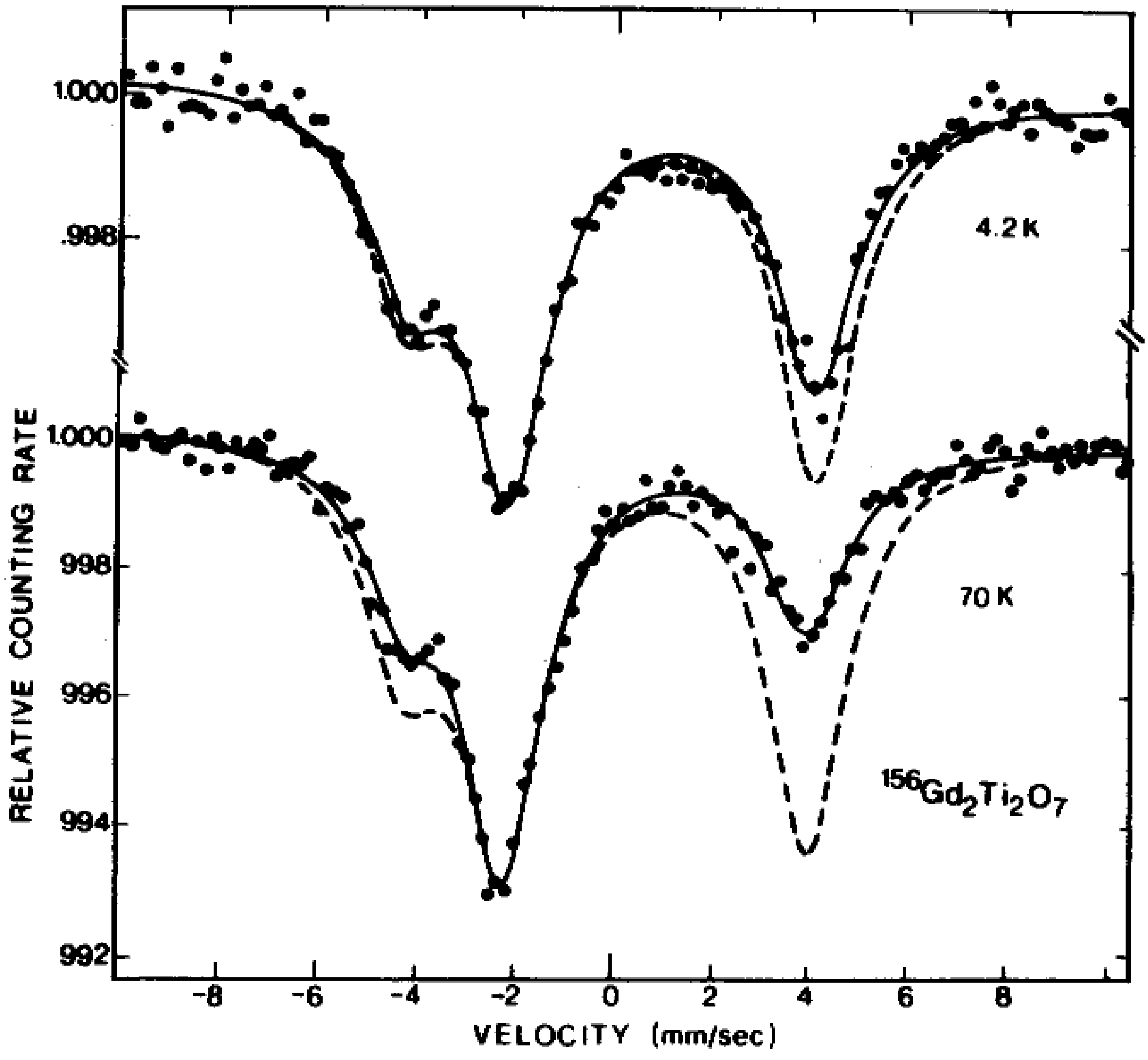

FIGURE 9. Recoilless absorption spectra of the 89-keV gamma rays of ^{156}Gd in $Gd_2Ti_2O_7$ at 4.2 and 70 K. The solid lines are the theoretical spectra obtained from a least-squares fit to the experimental spectra, taking into account an anisotropic absorption fraction. The dashed curves are the theoretical spectra obtained with an isotropic absorption fraction (from Reference 42).

To evaluate the reduction factors of the different transitions we start again with the component $\bar{r}_{11} = A_{00} + A_{20} + A_{40}$ of the absorber matrix of an $E2$ transition. The A_{Lm} have already been evaluated [equations (3.87a)–(3.87c)]. They are specified for the axial EFG tensor ($e_+ = 1$, $e_- = 0$). The absorber matrix components of degenerate states are summed up. The energies of the transitions are $E^1 = -6\mu_2$, $E^{2,3} = -3\mu_2$, and $E^{4,5} = 6\mu_2$ [equations (2.7) and (2.10)]. Inserting the super-texture components of a random powder the absorber matrix components $\bar{r}_{11}$ are given by

$$\begin{aligned} \bar{r}_{11}(\Delta m = 0) &= \frac{1}{5} + \frac{1}{35}\zeta_0^2 - \frac{12}{315}\zeta_0^4 \\ \bar{r}_{11}(\Delta m = \pm 1) &= \frac{2}{5} + \frac{1}{35}\zeta_0^2 + \frac{16}{315}\zeta_0^4 \\ \bar{r}_{11}(\Delta m = \pm 2) &= \frac{2}{5} - \frac{2}{35}\zeta_0^2 - \frac{4}{315}\zeta_0^4 \end{aligned} \tag{4.29}$$

If we extract the powder intensities (1/5, 2/5, and 2/5) and consider only relative intensities (thin absorber approximation) then the reduction factors B_0 and B_2 for the $\Delta m = 0$ and $\Delta m = \pm 2$ transitions, respectively, are the ratios

$$B_0 = \left(1 + \frac{1}{7}\zeta_0^2 - \frac{12}{63}\zeta_0^4\right) \Big/ \left(1 + \frac{1}{14}\zeta_0^2 + \frac{8}{63}\zeta_0^4\right) \tag{4.30a}$$

$$B_2 = \left(1 - \frac{1}{7}\zeta_0^2 - \frac{2}{63}\zeta_0^4\right) \Big/ \left(1 + \frac{1}{14}\zeta_0^2 + \frac{8}{63}\zeta_0^4\right) \tag{4.30b}$$

ζ_0^L is expressed by the reduction factors

$$\zeta_0^2 = 10(1 + B_0 - 2B_2)/(2 + B_0 + 2B_2) \tag{4.31a}$$

$$\zeta_0^4 = (9/2)\,(4 - 3B_0 - B_2)/(2 + B_0 + 2B_2) \tag{4.31b}$$

The values of B_0 and B_2 and the average Debye–Waller factor f obtained from the experiment are collected in Table 1. The anisotropy factors N are determined from the graphs of Figure 6 with the calculated values of ζ_0^2 and ζ_0^4. We expect that $N(\zeta_0^2)$ is the same as $N(\zeta_0^4)$. Suppose that the harmonic approximation is correct and we have a thin absorber; there is only one explanation left for the observed discrepancies [$N(\zeta_0^4) < N(\zeta_0^2)$] which are up to two standard deviations (for the measurement at $T = 70$ K): the presence of texture in the powder absorber. In the work of Armon *et al.*[42] the average values of N are presented. These are denoted